

Preparation and crystallization of chromium-based amorphous alloys

K. DINI, R. A. DUNLAP, P. HARGRAVES

Department of Physics, Dalhousie University, Halifax, Nova Scotia, B3H 3J5 Canada

The glass formability of the $\text{Cr}_{72}(\text{B}, \text{Si}, \text{C})_{25}\text{Al}_3$ system has been investigated. Samples were prepared by rapid quenching from the melt by the melt spinning technique. Of the compositions investigated, only $\text{Cr}_{72}\text{B}_{10}\text{C}_{10}\text{Si}_5\text{Al}_3$ and $\text{Cr}_{71}\text{C}_{17}\text{Si}_8\text{Al}_3$ formed fully amorphous alloys. These showed crystallization temperatures of 997 and 990 K, respectively, among the highest reported for transition metal-metalloid amorphous alloys. The crystallization products have been found to be Cr_7C_3 and $\text{Cr}_3(\text{Si}, \text{B})$ for $\text{Cr}_{72}\text{B}_{10}\text{C}_{10}\text{Si}_5\text{Al}_3$ and Cr_7C_3 and Cr_3Si for $\text{Cr}_{72}\text{C}_{17}\text{Si}_8\text{Al}_3$. The effects of substituting iron in place of chromium in $\text{Cr}_{72}\text{C}_{17}\text{Si}_8\text{Al}_3$ have been investigated. For up to 20 at% Fe the crystallization products are $(\text{Cr}, \text{Fe})_7\text{C}_3$ and Cr_3Si . An alloy with 30 at% Fe crystallizes into $(\text{Cr}, \text{Fe})_7\text{C}_3$ and hexagonal Cr-Si-C.

1. Introduction

Amorphous transition metal-metalloid alloys containing iron, nickel or cobalt as the principal transition metal have commonly been prepared by rapid quenching from the melt. Investigations of iron-based alloys into which chromium has been substituted for up to approximately 35% of the iron have been reported by a number of authors (e.g. [1-8]). These alloys are of interest, as the addition of chromium decreases the Curie temperature much faster than would be expected on the basis of percolation and in a region around 30% Cr the alloys exhibit spin glass behaviour [3, 4]. From a commercial viewpoint, the addition of chromium to iron-based alloys is of interest, as this has been found to both increase the crystallization temperature [1, 6, 7] and improve the corrosion resistance [2]. For alloys of the composition $\text{Fe}_{80-x}\text{Cr}_x(\text{B}, \text{Si})_{20}$ the concentration of chromium is limited to about 35 at%. The phase diagrams of several binary chromium-metalloid alloys show eutectics (see e.g. [9]), which suggest the possibility of forming an amorphous phase. The melting temperatures, however, of these eutectic compositions are typically too high to permit the use of the conventional melt spinning technique. In this work we have investigated the possibility of preparing chromium-based amorphous alloys using a combination of metalloids. The system which we have studied is $\text{Cr}_{72}(\text{B}, \text{C}, \text{Si})_{25}\text{Al}_3$. In addition, the effect of iron substituting for chromium in $\text{Cr}_{72-x}\text{Fe}_x\text{C}_{17}\text{Si}_8\text{Al}_3$ has been investigated. Differential thermal analysis measurements have been made to determine the crystallization temperature, and X-ray diffraction measurements were used to identify the resultant crystalline phases. A preliminary investigation of the glass formability in chromium-metalloid alloys has been reported previously [10].

2. Sample preparation and experimental methods

Alloys have been rapidly quenched by melt spinning.

Melts were ejected from a quartz tube through a 0.5 mm orifice by 110 kPa of argon on to the surface of a 15 cm diameter copper roller rotating at approximately 6000 r.p.m. Resulting ribbons were approximately 1 mm wide by 15 μm thick. The structure of the as-quenched ribbons, as well as the crystalline phases present in partially and fully crystallized samples, was investigated by X-ray diffraction measurements performed on a Siemens scanning diffractometer using $\text{MoK}\alpha$ radiation. The details of the crystallization processes were determined by differential thermal analysis (DTA) measurements. These measurements were performed on a Fisher model 260F thermal analyser, modified to enable the sample to be heated under an argon atmosphere [11]. This permitted measurements to be made up to about 1500 K. All DTA measurements were made using a heating rate of 20 K min^{-1} . All partially and fully crystallized samples used in the X-ray studies were heated at this same rate. DTA measurements were made on samples of approximately 25 mg.

3. Results and discussion

3.1. Glass formability of chromium-metalloid alloys

A variety of compositions in the system $\text{Cr}_{72}(\text{B}, \text{S}, \text{Si})_{25}\text{Al}_3$ have been prepared. Fig. 1 shows the alloys which were investigated and the characteristics of the as-quenched alloys. These fall into three categories: (1) those which formed fully amorphous ribbons; (2) those which formed partially crystalline ribbons, and (3) those which did not form ribbons. The last category resulted from alloys which had excessively high melting temperatures or which did not flow properly when melted and, as a result, did not form ribbons. We see that only the compositions $\text{Cr}_{72}\text{B}_{10}\text{C}_{10}\text{Si}_5\text{Al}_3$ and $\text{Cr}_{72}\text{C}_{17}\text{Si}_8\text{Al}_3$ could be formed in the fully amorphous state. On the basis of Fig. 1 it is presumed that only compositions near these two will form amorphous ribbons. Both these compositions

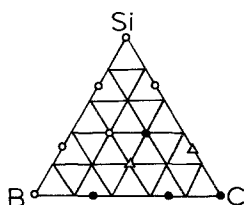


Figure 1 Phase diagram of the $\text{Cr}_{72}(\text{B}, \text{C}, \text{Si})_{25}\text{Al}_3$ system. The glass formability is indicated by (Δ) formed amorphous ribbons, (\bullet) formed partially crystalline ribbons, and (\circ) did not form ribbons.

were found to have melting temperatures of approximately 1650 K, as measured by a Leeds and Northrup model 8622-C optical pyrometer. Alloys of the composition $\text{Cr}-(\text{B}, \text{C}, \text{Si})$ without the small quantity of aluminium, could with somewhat greater difficulty, be formed into amorphous ribbons. The physical quality of these ribbons was much worse and it appears that the small amount of aluminium is significant in improving glass formability. This is, perhaps, as a result of a reduction in the viscosity of the melt.

3.2. Crystallization of chromium-based amorphous alloys

Fig. 2 shows DTA scans of $\text{Cr}_{72}\text{B}_{10}\text{C}_{10}\text{Si}_5\text{Al}_3$ and $\text{Cr}_{72}\text{C}_{17}\text{Si}_8\text{Al}_3$. The scans are similar and show a small exothermic reaction followed by a much larger exothermic reaction at slightly higher temperature. The temperature of the onset of these peaks is given in Table I. We see that the temperature of the onset of the lower temperature exotherm is similar but that there is a somewhat larger difference in the temperature of the higher temperature exotherm. As shown in the table, the crystalline phases in the fully crystallized samples are Cr_7C_3 and $\text{Cr}_3(\text{Si}, \text{B})$ for $\text{Cr}_{72}\text{C}_{10}\text{Si}_5\text{Al}_3$ and Cr_7C_3 and Cr_3Si for $\text{Cr}_{72}\text{C}_{17}\text{Si}_8\text{Al}_3$. The Cr_7C_3 phase is hexagonal with $a = 1.398$ nm and $c = 0.4523$ nm [12–14], while the Cr_3Si phase is cubic with $a = 0.4558$ nm [15, 16]. The boron in $\text{Cr}_{72}\text{B}_{10}\text{C}_{10}\text{Si}_5\text{Al}_3$ is believed to go primarily into the Cr_3Si phase, as this phase shows a slightly smaller lattice parameter than the same phase in crystallized $\text{Cr}_{72}\text{C}_{17}\text{Si}_8\text{Al}_3$. The crystallographic location of the aluminium could not be determined. In order to determine the identity of the two peaks in the DTA scans, samples of the two compositions were heated to 1038 K, followed by quenching into water. The quenching is to ensure that the crystallization process responsible for the higher temperature exotherm does not begin. In both cases the X-ray pattern indicates that the principal phase is still amorphous, but that a small quantity of crystalline Cr_7C_3 is present as well. Thus the higher temperature exotherm represents the formation of a phase with the Cr_3Si structure. The

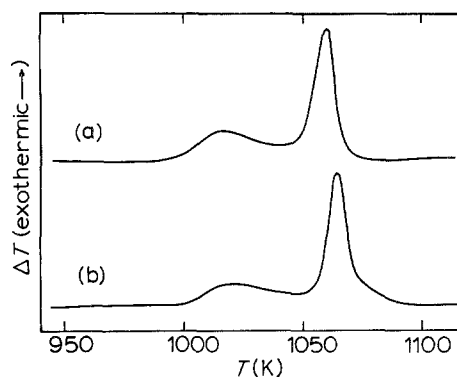


Figure 2 DTA scans for the alloys: (a) $\text{Cr}_{72}\text{B}_{10}\text{C}_{10}\text{Si}_5\text{Al}_3$ and (b) $\text{Cr}_{72}\text{C}_{17}\text{Si}_8\text{Al}_3$.

results are summarized in Table I. These observations are consistent with the conclusion that the boron is included in the Cr_3Si phase. Hence it is the temperature of the crystallization of this phase, rather than the Cr_7C_3 phase, as shown in Table I, which is affected most by the change in the composition of the alloy.

3.3. Effects of iron on the crystallization

We have chosen the simpler of the two metalloid compositions to investigate the effects of iron on the crystallization. Five fully amorphous alloys with compositions $\text{Cr}_{72-x}\text{Fe}_x\text{C}_{17}\text{Si}_8\text{Al}_3$ with $5 < x < 30$ have been prepared. DTA scans of the five alloys are shown in Fig. 3.

We can compare the scans with that shown in Fig. 2 for the $\text{Cr}_{72}\text{C}_{17}\text{Si}_8\text{Al}_3$ sample. A clear progression is observed for alloys with $x < 20$. The $x = 30$ alloy is considered separately below. For $x = 0$ and $x = 5$ the DTA scans show a small peak followed by a larger peak at higher temperature. As the iron content increases, the temperature of the lower temperature peak increases relative to that of the higher temperature peak. For the $x = 15$ sample, the peaks occur at essentially the same temperature. Values of the temperature of the onset of the two exothermic peaks are given in Table II.

X-ray diffraction measurements of fully crystallized samples with $5 < x < 20$ show the presence of a Cr_7C_3 phase and a Cr_3Si phase. Both phases show lattice parameters which are in agreement with reported values [14, 15] and are essentially unchanged from those observed in the crystallized $\text{Cr}_{72}\text{C}_{17}\text{Si}_8\text{Al}_3$ sample. On the basis of this observation, it is probable that the additional iron has gone into the Cr_7C_3 phase, as Goldschmidt [16] has reported that, at least up to a certain iron content, the lattice parameter of $(\text{Cr}, \text{Fe})_7\text{C}_3$ is independent of stoichiometry.

As previously discussed, the lower temperature

TABLE I Results of the crystallization study of $\text{Cr}_{72}\text{B}_{10}\text{C}_{10}\text{Si}_5\text{Al}_3$ and $\text{Cr}_{72}\text{C}_{17}\text{Si}_8\text{Al}_3$

| Alloy | Crystallization temperatures (K) | | Crystalline phases present | |
|--|----------------------------------|--------------|----------------------------|--|
| | T_1 | T_2 | heated to 1038 K | fully crystalline |
| $\text{Cr}_{72}\text{B}_{10}\text{C}_{10}\text{Si}_5\text{Al}_3$ | 997 ± 3 | 1047 ± 3 | Cr_7C_3 | $\text{Cr}_7\text{C}_3 + \text{Cr}_3(\text{Si}, \text{B})$ |
| $\text{Cr}_{72}\text{C}_{17}\text{Si}_8\text{Al}_3$ | 990 ± 3 | 1061 ± 3 | Cr_7C_3 | $\text{Cr}_7\text{C}_3 + \text{Cr}_3\text{Si}$ |

TABLE II Crystallization temperatures for the alloys $\text{Cr}_{72-x}\text{Fe}_x\text{C}_{17}\text{Si}_8\text{Al}_3$. T_1 is the temperature of the onset of the small exotherm and T_2 is the temperature of the onset of the larger exotherm

| x | T_1 (K) | T_2 (K) |
|-----|-----------|-----------|
| 0 | 990 | 1061 |
| 5 | 1018 | 1058 |
| 10 | 1049 | 1061 |
| 15 | 1040 | 1040 |
| 20 | 1030 | 1019 |
| 30 | 955 | 986 |

exotherm for the $x = 0$ sample represents the formation of Cr_7C_3 . For most of the iron-containing alloys, the overlap of the two exotherms prevents a definitive analysis of the identity of each peak. On the basis of the trends shown in Fig. 3, however, it seems reasonable to assume that the smaller exotherm corresponds to the crystallization of $(\text{Cr}, \text{Fe})_7\text{C}_3$, while the larger peak corresponds to the crystallization of Cr_3Si . The trend is illustrated in Fig. 4.

An X-ray diffraction pattern of the fully crystallized $x = 30$ sample shows the presence of $(\text{Cr}, \text{Fe})_7\text{C}_3$ and CrSiC . This latter compound is hexagonal with $a = 0.6993 \text{ nm}$ and $c = 0.4725 \text{ nm}$ [17]. A sample was heated to 975 K, above the lowest temperature exotherm, and quenched into ice-water. An X-ray diffraction pattern of this sample showed the presence of an amorphous phase and a quantity of $(\text{Cr}, \text{Fe})_7\text{C}_3$, indicating that this is the crystalline phase which precipitates at the lower temperature.

It is interesting to note that small amounts of iron substituting for chromium in $\text{Cr}_{72}\text{C}_{17}\text{Si}_8\text{Al}_3$ actually increase the crystallization. As Fig. 4 shows, however, this trend reverses at more than 10 to 15 at % Fe. This is in contrast with several previous investigations

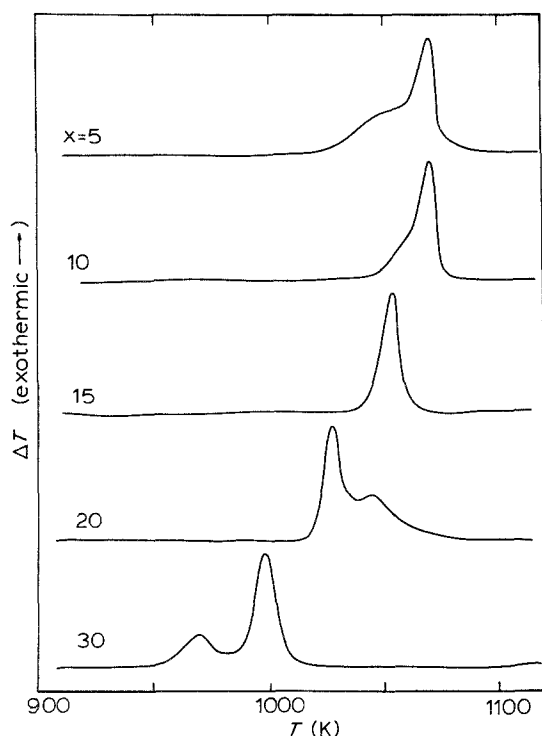


Figure 3 DTA scans for the alloys $\text{Cr}_{72-x}\text{Fe}_x\text{C}_{17}\text{Si}_8\text{Al}_3$ for $5 < x < 30$.

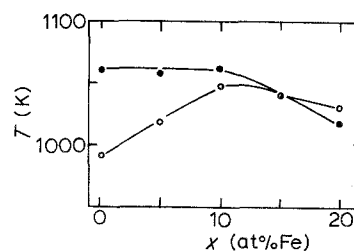


Figure 4 Crystallization trends in $0 < x < 20$ alloys. T_1 is given by (○) and T_2 by (●).

which indicate that chromium substituted into iron-based alloys increases the crystallization temperature [1, 6, 7, 18]. This trend in these and other substituted alloys has been attributed to differences in the atomic volumes of the transition metals [1, 5]. It should be pointed out that some other studies have found that chromium additions have little effect on the crystallization temperature of iron-based alloys [5, 8]. Some of the differences observed in crystallization studies may result from variations in the metalloid compositions or, as has been suggested by Walter [5], from differences in the total amount of transition metals in the alloys.

Although the present study shows that the crystallization in the chromium-based alloys occurs at higher temperatures than in iron-based alloys, it is shown that it is not reasonable to assume that the change in the crystallization temperature should show monotonic dependence on alloy composition. This is shown to be true, from Fig. 4, even over ranges of composition where there is no significant change in the crystallization products. It may be important, however, that the largest change in crystallization temperature, i.e. $\partial T_1 / \partial x$, occurs over the range of compositions where there is also a change in the identity of the crystalline products.

Acknowledgements

This work was supported by a grant from the Natural Sciences and Engineering Research Council of Canada. The authors are grateful for technical assistance provided by P. Sinclair and B. Fullerton.

References

1. R. A. DUNLAP, J. E. BALL and K. DINI, *J. Mater. Sci. Lett.* **4** (1985) 773.
2. R. B. DIEGLE, *J. Non-cryst. Solids* **61-62** (1984) 601.
3. M. OLIVIER, J. O. STÖM-OLSEN, Z. ALTOUNIAN and G. WILLIAMS, *J. Appl. Phys.* **53** (1982) 7696.
4. YU BOLIANG, J. M. D. COEY and J. O. STRÖM-OLSEN, *ibid.* **55** (1984) 1748.
5. J. L. WALTER, *Mater. Sci. Eng.* **50** (1981) 137.
6. I. W. DONALD and H. A. DAVIS, in "Proceedings of the 3rd International Conference on Rapidly Quenched Metals" (The Metals Society, London, 1978) p. 273.
7. W. S. CHAN, B. G. SHEN, H. Y. LO and B. L. YU, in "Proceedings of the 4th International Conference on Rapidly Quenched Metals" (Japan Metals Society, Sendai, 1981) p. 1137.
8. H. J. VIND NIELSON, *J. Magn. Magn. Mater.* **12** (1979) 187.
9. M. HANSEN, "Constitution of Binary Alloys" (McGraw-Hill, New York, 1958) p. 247.
10. R. A. DUNLAP, P. SINCLAIR, P. HARGRAVES,

- K. DINI and S. JHA, 1985 International Magnetics Conference (INTERMAG) St Paul, Minnesota.
11. K. DINI, R. A. DUNLAP and G. STROINK, *J. Phys. F, Met. Phys.* **14** (1984) 2009.
 12. A. WESTGREN, *Jernkontorets Ann.* **119** (1935) 231.
 13. D. S. BLOOM and N. J. GRANT, *Trans. AIME* **188** (1950) 41.
 14. P. STECHER, F. BENESOVSKY and H. NOWOTNY, *Planseeber. Pulvernet.* **12** (1964) 89.
 15. R. KIEFFER, F. BENESOVSKY and H. SCHROTH, *Z. Metallkde* **44** (1953) 437.
 16. H. J. GOLDSCHMIDT, *Metallurgica* **40** (1949) 103.
 17. E. PARTHÉ, H. SCHACHNER and H. NOWOTNY, *Montash. Chem.* **86** (1955) 182.
 18. M. NAKA, S. TOMIZAWA, T. WATANABE and T. MASUMOTO, in "Proceedings of the 2nd International Conference on Rapidly Quenched Metals" (MIT Press, Cambridge, Massachusetts, 1976) p. 273.

*Received 3 April
and accepted 28 May 1985*